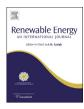


Contents lists available at ScienceDirect

Renewable Energy

journal homepage: www.elsevier.com/locate/renene



Microgrid capability diagram: A tool for optimal grid-tied operation



A.V. Jayawardena, L.G. Meegahapola*, D.A. Robinson, S. Perera

Australian Power Quality and Reliability Centre, School of Electrical, Computer and Telecommunications Engineering, University of Wollongong, Wollongong, New South Wales 2522, Australia

ARTICLE INFO

Article history:
Received 5 November 2013
Accepted 14 August 2014
Available online 13 September 2014

Keywords:
Capability diagram
Distributed generation
Distribution system
Grid-tied microgrid
Optimisation

ABSTRACT

The microgrid paradigm has gained much interest in the electricity industry due to the increased penetration of distributed resources. A grid-tied microgrid can be viewed as a single generating entity or a load depending on its power export and import at the grid supply point. Similar to conventional generators, grid-tied microgrids have the potential to be able to participate in the energy market in the future to achieve technical, financial and environmental benefits. Effective participation in the energy markets requires numerous planning tools and a comprehensive understanding of the full capability of the microgrid. This paper presents a systematic approach for developing a capability of a grid-tied microgrid which represents the active and reactive power exchange capability of the microgrid with the main grid. Capability diagrams have been developed for two different microgrids and the impacts of different modelling aspects and network conditions have been analysed using several case studies. Effects of plug-in hybrid electric vehicles, capacitor banks, and other storage devices on microgrid capability diagram have also been addressed in this paper. Furthermore, operating points of the capability diagram have been verified using time domain simulations.

© 2014 Elsevier Ltd. All rights reserved.

1. Introduction

Increasing penetration of localised energy generation (PV systems, wind generators, micro-turbines etc.), and storage devices (batteries, flywheels etc.) at distribution level has payed the way for the microgrid paradigm to become a reality. Integration of multiple microgrids into the utility grid will allow microgrids to provide ancillary services to the utility during normal operation and to provide emergency services to adjacent microgrids during a main grid outage. Besides technical and financial benefits, due to being an enabler of renewable and high efficiency distributed generation resources, operation of microgrids can also provide environmental benefits by reducing the overall carbon footprint and creating zeronet-energy communities [1]. Grid-tied microgrids can behave as single generating units or as loads in a technically and economically feasible way. Similar to the large generators in traditional power systems, microgrids could participate in wholesale markets to supply energy and other ancillary services to the network in the future [2].

Few research activities have been carried out on developing microgrid central control systems for a multi-microgrid environment. In Ref. [3], optimal resource allocation within the microgrid is carried out by a microgrid central controller (MCC) and it has been assumed that there is no limit to the power exchanged with the main grid. Participation of microgrids in the open market has been considered in Ref. [4] which enable microgrids to trade power with the main grid. However, in Refs. [3,4], the distribution network service provider (DNSP) or the distribution management system is unable to obtain the overall active and reactive power capabilities of the microgrid within the technical constraints for the considered time interval. Most of the research in this area has been focused on optimising the power availability and minimising operation costs within the distribution network while minimising power flow through the grid supply point (GSP) [5-8]. Allowing grid-tied microgrids to participate in energy and ancillary service markets while fulfilling the local energy demand will provide opportunity for additional revenue for the microgrids, however, considerable planning and understanding of the technical capabilities of the microgrid as an energy resource is required. In order to enable this operation and to make decisions in the market, MCCs and DNSPs must not only find the optimum operating conditions, but they must also be aware of the full capability of the microgrid at the GSP.

Capability diagrams are considered essential system planning tools and are widely used in power system operation. The concept

^{*} Corresponding author. Tel.: +61 242213408; fax: +61 242213236.

E-mail addresses: avj998@uowmail.edu.au (A.V. Jayawardena), lasantha@ieee.
org, lasantha@uow.edu.au (L.G. Meegahapola), duane@uow.edu.au
(D.A. Robinson), sarath@uow.edu.au (S. Perera).

of the capability diagram is traditionally related to synchronous machines, and represents the area of permissible operation in terms of active and reactive power available at the machine terminal [9,10]. Recent research has been carried out on developing capability diagrams for wind turbine based doubly-fed-induction-generator (DFIG) [11,12], grid connected PV units [13], generator—transformer units [14], and for HVDC links [15]. A graphical method to determine the network limits of a wind farm is presented in Ref. [16]. For a multiple node system, the capability diagram is obtained by reducing the network into a two-node system and using Thevenin's equivalent for the system at the particular node of interest. However, practicability of this method reduces with the increasing size of the network.

The total load supplying capability of a power system is modelled and represented as a capability diagram in Ref. [17] using an optimisation approach subjected to technical and operating constraints. In Ref. [18], reactive power support from networks comprising only voltage controlling wind generators has been analysed, where a P—Q capability diagram has been derived without taking the local loads into account. Deriving a diagram for the maximum power transfer capability of a grid-tied microgrid is much different from individual distributed generators (DGs) or wind farms due to the complexity of the microgrid, caused by the network configuration, network constraints and the combination of different DGs and loads.

This paper introduces a new approach of developing an active and reactive power capability diagram corresponding to the GSP of a microgrid, while considering microgrid generation capabilities. local load demand and network constraints. Various features such as different load modelling aspects, individual machine limitations, and effects of plug-in hybrid electric vehicles (PHEVs) and reactive power devices are considered in developing the capability diagram. Capability diagrams are derived based on an optimisation model in MATLAB for two different microgrid models, which are validated using DIgSILENT PowerFactory. This graphical representation of the active and reactive power capability at the GSP can be utilised as a new tool for grid-tied microgrids in market operation. This tool is required to assist in understanding the full capability of a microgrid, to allow optimum use of distributed energy resource (DERs), and to provide coordinated support to the network through ancillary services as required.

Structure of the paper is as follows; Section 2 presents the optimisation model and development of a simplified capability diagram for an example microgrid. Derivation of a more detailed and realistic capability diagram with various case studies are presented in Section 3. Impacts of the operation of PHEVs, storage devices, and capacitor banks on microgrid capability are presented in Section 4. Discussion and conclusions are given in Section 5 and Section 6 respectively.

2. Development of microgrid capability diagram

2.1. Non-linear optimisation model

In this section, the development of a capability diagram is demonstrated for a grid-tied microgrid. The capability diagram is derived using the optimisation technique. Objective function for the optimisation model is developed so as to maximise the active power flow through the GSP while minimising the active power losses in the microgrid.

Objective function;

$$\operatorname{Max}\left(P_{\operatorname{GDP}} - \sum P_{\operatorname{loss}}\right) \tag{1}$$

where P_{GSP} is the active power through the grid supply point and $\sum P_{\text{loss}}$ is the total active power loss in the microgrid.

The objective function is subjected to the general load flow equalities expressed in (2) and (3).

$$P_{gi} - P_{li} - P_i(V, \delta) = 0 \tag{2}$$

$$Q_{\sigma i} - Q_{li} - Q_i(V, \delta) = 0 \tag{3}$$

where $P_{\rm gi}$, $Q_{\rm gi}$ are the active and reactive power outputs from the generator at node i, $P_{\rm li}$, $Q_{\rm li}$ are the active and reactive power demands of the load at node i, and P_{i} , Q_{i} are the active and reactive power flow through node i.

$$P_i(V,\delta) = V_i \sum V_k Y_{ik} \cos(\delta_i - \delta_k - \emptyset_{ik})$$
(4)

$$Q_{i}(V,\delta) = V_{i} \sum V_{k} Y_{ik} \sin(\delta_{i} - \delta_{k} - \emptyset_{ik})$$
(5)

where \emptyset_{ik} is the phase angle of the line admittance between node i and node k, δ_i is the phase angle of the voltage at nodes i with respect to the reference node, V_i is the magnitude of the voltage at node i, and Y_{ik} is the magnitude of the line admittance between node i and node k.

The capability diagram is derived while maintaining all the network voltages and line currents within the rated values. Inequalities which will account for the limits on magnitude and phase angle of nodal voltages are given by (6) and (7);

$$V_i^{\min} \le V_i \le V_i^{\max} \tag{6}$$

$$-\pi \le \delta_i \le \pi \tag{7}$$

Distribution line capacity limit is given by;

$$I_{ik}(V,\delta) \le I^{\max} \tag{8}$$

where I_{ik} is the magnitude of the current flow from node i to node k;

$$I_{ik}(V,\delta) = \frac{\sqrt{V_i^2 + V_k^2 - 2V_iV_k\cos\left(\delta_i - \delta_k\right)}}{Z_{i\nu}}$$
(9)

where Z_{ik} is the magnitude of the line impedance between node i and node k.

Power flow between the microgrid and the main grid is limited by the rating of the coupling transformer at the GSP. Thus, the transformer power limit is incorporated using (10);

$$\sqrt{P_{tr}^2 + Q_{tr}^2} \le S_{tr} \tag{10}$$

where S_{tr} is the rated apparent power of the transformer.

Furthermore, the maximum and minimum generator power capability limits are incorporated in to the optimisation model by;

$$Q_{gi}^{min} \le Q_{gi} \le Q_{gi}^{max} \tag{11}$$

$$P_{gi}^{\min} \le P_{gi} \le P_{gi}^{\max} \tag{12}$$

Reactive power through the GSP is increased iteratively using (3), and the optimisation model is solved at each step to obtain the maximum active power flow through the GSP. This procedure is carried out for both power import and export modes in order to develop the complete capability diagram while the objective function is subjected to typical AC power flow constraints

Download English Version:

https://daneshyari.com/en/article/300001

Download Persian Version:

https://daneshyari.com/article/300001

<u>Daneshyari.com</u>